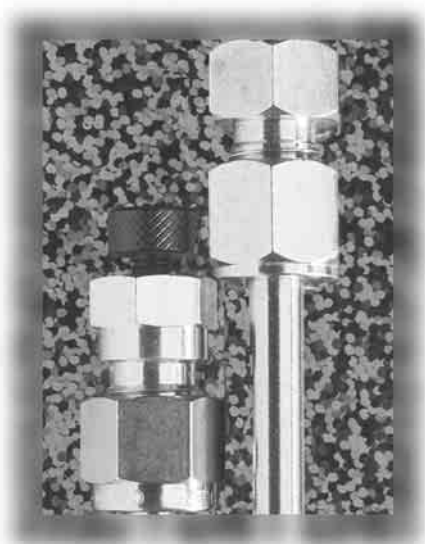# Analytical Advantages of Highly Stable Stationary Phases for Reversed-Phase LC

During the past five years, many manufacturers of high performance liquid chromatography (HPLC) columns have focused on improving stationary-phase stability and reproducibility. Improved column stability — both chemical and thermal — offers new advantages, such as decreased analysis time and new methods of selectivity optimization. More stable HPLC packing materials have been achieved through advances in silane chemistry; however, the greatest improvements in stability have resulted from the use of alternative nonsilica supports such as synthetic organic polymers, alumina, and zirconia. In this article, the authors describe their use of various test solutes to compare the efficiency, selectivity, and hydrophobic retention mechanisms of five commercially available HPLC columns based on silica, alumina, zirconia, and polystyrene cross-linked with divinylbenzene (PS–DVB).

Clayton McNeff,
Lorinda Zigan,
Kerry Johnson, Peter W. Carr,
Aosheng Wang*, and
Anne M. Weber-Main†
ZirChrom Separations Inc.,
617 Pierce Street, Anoka,
Minnesota 55303
* University of Minnesota,
207 Pleasant Street, Minneapolis,
Minnesota 55455
† University of Minnesota,
1288 Schletti Street, St. Paul,
Minnesota 55117

*Address correspondence to
C. McNeff.*

Reversed phase continues to be the dominant mode of high performance liquid chromatography (HPLC) because of the wide range of chemically diverse compounds that can be analyzed by this technique and the large body of reversed-phase liquid chromatography (LC) literature, which greatly facilitates the development of new analyses. Historically, silica gel has been the support material of choice for producing reversed-phase stationary phases. Silica's flexible chemical surface enables easy modification through a diverse range of silane chemistry. In addition, its wide range of particle and pore sizes, monodispersity, mechanical stability, and good mass transfer properties have promoted silica's dominant position in LC.

Analytical advantages of pH and thermal stability: Recent research about silica-based stationary phases largely has focused on exploiting the bonding chemistry and improving the chemical and thermal stability of the base silica (1,2). This work is rooted in practicality: enhanced pH and thermal stability of reversed-phase LC packing materials allows for the widest possible range of chromatographic conditions that can be exploited (see Figure 1). For example, chromatographers can use high pH to suppress amine protonation and low pH to suppress the ionization of acidic solutes. Extreme chemical stability also enables the cleaning of fouled columns under very acidic conditions and the sterilization or depyrogenation of columns with alcoholic basic solutions. By using low-pH conditions, analysts can increase the retention of anions by protonating them, thereby avoiding the need for quaternary amine ion-pairing agents. Similarly, one can, in principle, increase the retention of positively charged amines by raising the pH to higher than the pK_a of the protonated Brönsted acid. Unfortunately, the pH required to fully protonate many carboxylic acids and completely deprotonate aliphatic amines lies outside the stable range (pH 2–8) of silica-based phases (3).

Thermal column stability has its own distinct inherent advantages (see Figure 1). It can enable analyses at higher column temperatures, which lower mobile-phase viscosity and lessen the mechanical wear and tear on LC pumping systems. Higher run temperatures also lower the retention of solutes in reversed-phase mode, and this process often results in

faster analyses or the ability to reduce the necessary amount of organic modifier to elute the solutes. Antia and Horváth (4) performed a series of detailed analytical calculations regarding the potential benefits of using high temperature to bring about significant, even 10-fold reductions in analysis time. Their work predicts a considerable decrease in time of analysis with an increase in column temperature, while maintaining a constant pressure drop by increasing flow rate or decreasing the column length. Of course, analysis speed also is limited by the decrease in plate count at higher linear velocities. The thermal stability of a column is beneficial: an increase in column temperature actually helps to improve the column efficiency at high velocities by increasing the rate of solute diffusion into and out of the stationary-phase particle, thereby decreasing the peak width (5,6).

With thermal stability comes the freedom to use column temperature to optimize the separation, which can lead to a more robust separation or to beneficial selectivity changes. For example, Snyder and co-workers (7,8) recently showed that temperature, when used in conjunction with adjustments in mobile-phase composition, can be a very powerful aid in optimizing separations even with stationary phases that have upper temperature limits of only 80–90 °C. Thermal stability also can make method development easier because temperature is easily changed, whereas mobile-phase changes may require long equilibration periods after switching between drastically different organic modifiers.

Another driving force for the recent interest in high-temperature HPLC is the concern for performing green chemistry and minimizing or eliminating toxic waste generation. Building on Hawthorne, Yang, and Miller's (9) work using supercritical water, Smith and Burgess (10,11) used subcritical water (at temperatures as high as 210 °C) with no organic modifier to separate both polar and hydrophobic species, including priority phenols and drugs on polymer reversed-phase media. They showed that UV detection could be performed even at a very short wavelength of 190 nm; thus, many species that do not absorb at longer wavelengths can be detected easily. Similarly, Miller and Hawthorne (12) showed that a flame ionization detector can be used with pure water as the eluent. The boiling point of water is approximately 200 °C at 20 bar, so a small back pressure will prevent boiling. An octadecylsilane, or C18, col-

umn, however, proved to be too unstable to be used on a practical time scale, even in pure water at temperatures of only 120 °C. Indeed, the typical commercial alkyl silane–bonded silica phase is seldom used at more than 20–30 °C higher than room temperature because of its instability at higher temperatures, especially in phosphate buffers (13–22).

The advent of more stable phases for reversed-phase LC: Recent advances in silane chemistry have led to the development of more stable silica-based phases (1,2). However, even greater strides in thermal and chemical stability have been achieved through alternatives to silica gel, including synthetic organic polymers (15–18), alumina (3,13,14,23), and zirconia (24–39). Zirconia-based columns have received a great deal of attention recently because of their extraordinary stability under extreme thermal and chemical conditions (40–42). Figure 2 demonstrates zirconia's chemical stability compared with that of other metal oxides (43). Zirconia shows no detectable dissolution across the entire pH range during 15 days of exposure, whereas a significant amount of alumina is dissolved under the same conditions. The chemical stability contrast between zirconia and silica would be even greater, because silica is more soluble than alumina at pH levels higher than neutral.

When coated with a thin layer of polybutadiene, zirconia becomes a reversed phase that is able to withstand extended exposure to mobile phases at pH 14 at a flow rate of 1 mL/min (Figure 3a) and column temperatures as high as 200 °C (Figure 3b). The extraordinary thermal stability of this type of column enables rapid analysis of a series of chlorophenols at 200 °C in a purely aqueous mobile phase (Figure 4). At low column

temperatures (such as 30 °C), an organic modifier is needed to elute the chlorophenols from the column (Figure 4a). As the column temperature is increased to 80 °C, the retention time of the last eluting solute is more than halved at the same flow rate (Figure 4b). At 200 °C, the separation is achieved quickly and without any organic modifier (Figure 4c).

As a final illustration, Figure 5 shows the separation of a series of tricyclic antidepressants on a polybutadiene-coated zirconia phase compared with that on a conventional C18 silica phase. The chromatogram acquired using the zirconia column shows much better peak symmetry and efficiency. Moreover, the separation on the polybutadiene-coated zirconia phase column was achieved in less than half the time required by the one on the silica column and at pH 12, which is inaccessible on conventional C18 silica phases.

As HPLC column manufacturers continue to develop more stable and reproducible stationary phases, chromatographers who must choose from these columns can benefit from a comparison of column performance properties. In our study, we examined the reversed-phase selectivity and efficiency of five of the most stable types of reversed-phase stationary phases currently available. They included a prototypical silica-based phase (C18 silica); a purely polymeric phase; two polymer-coated metal oxide phases, one based on alumina and one on zirconia; and last, a graphitized carbon–clad zirconia phase that has very similar chromatographic selectivity to that of the Hypercarb phase (ThermoQuest Chromatography Supplies, Runcorn, United Kingdom) (44). We also looked more closely
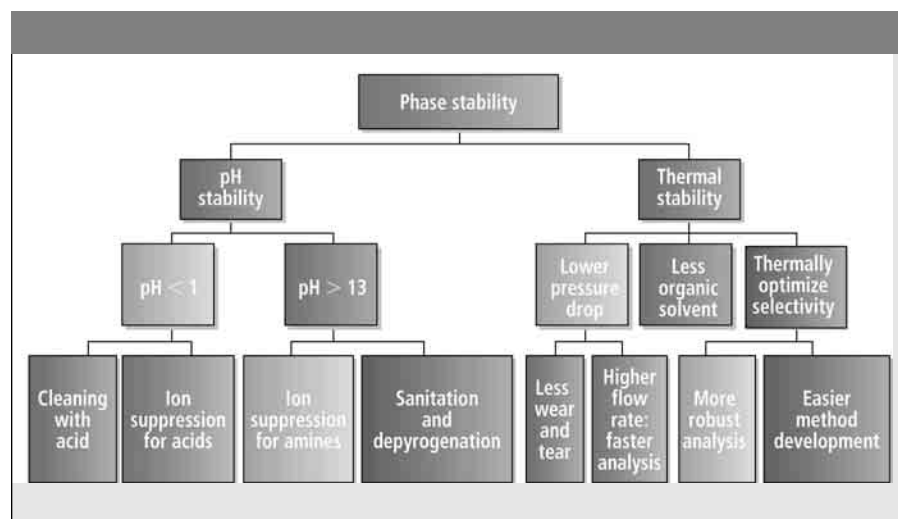
Figure 1: Benefits of chemical (pH) and thermal stationary-phase stability for reversed-phase HPLC analyses.
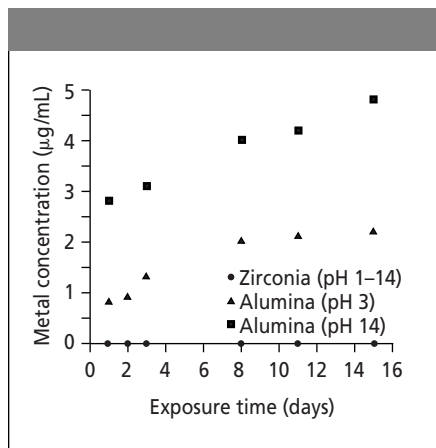
Figure 2: Comparison of pH stability of zirconia and alumina phases as analyzed by inductively coupled plasma spectroscopy (43).

at the retention mechanisms of these five phases by examining the hydrophobic interactions of each with a homolog series of alkylbenzenes and by performing a principal component analysis of retention data for 21 test analytes.

Experimental

Table I lists the general characteristics of the five columns under study, including their particle and pore sizes, column dimensions, low and high pH limits, and temperature limits. To assess their reversed-phase selectivity and efficiency, we chose 27 probe analytes to cover a wide range of solute–stationary-phase interactions; Table II lists these compounds.

We chose mobile-phase conditions for the efficiency and selectivity experiments that were similar to those used in a previous study, which tested 86 different silica-based reversed-phase columns with six probe analytes (45). The mobile phase was 40:60 (v/v) acetonitrile–buffer (50 mM phosphate buffer at pH 3.2) with a flow rate of 1.0 mL/min. The column temperature was 21 °C. We used UV detection at 254 nm. All chemicals were reagent grade or better. All chromatograms were collected on an Agilent Technologies 1100 chromatograph (Wilmington, Delaware) equipped with a variable-wavelength UV detector, and data were collected using Agilent Technologies ChemStation software. We used uracil as the dead volume marker for all chromatographic investigations.

We performed principal component analysis using the singular value decomposition function from Matlab 5.2 software (Math Works Inc., Natick, Massachusetts). To remove differences in log k values caused by the unique phase ratio of each column, we determined the mean center of the log k values from each column before the analysis. The number of principal components was determined by a comparison of the residual standard deviation with the esti-
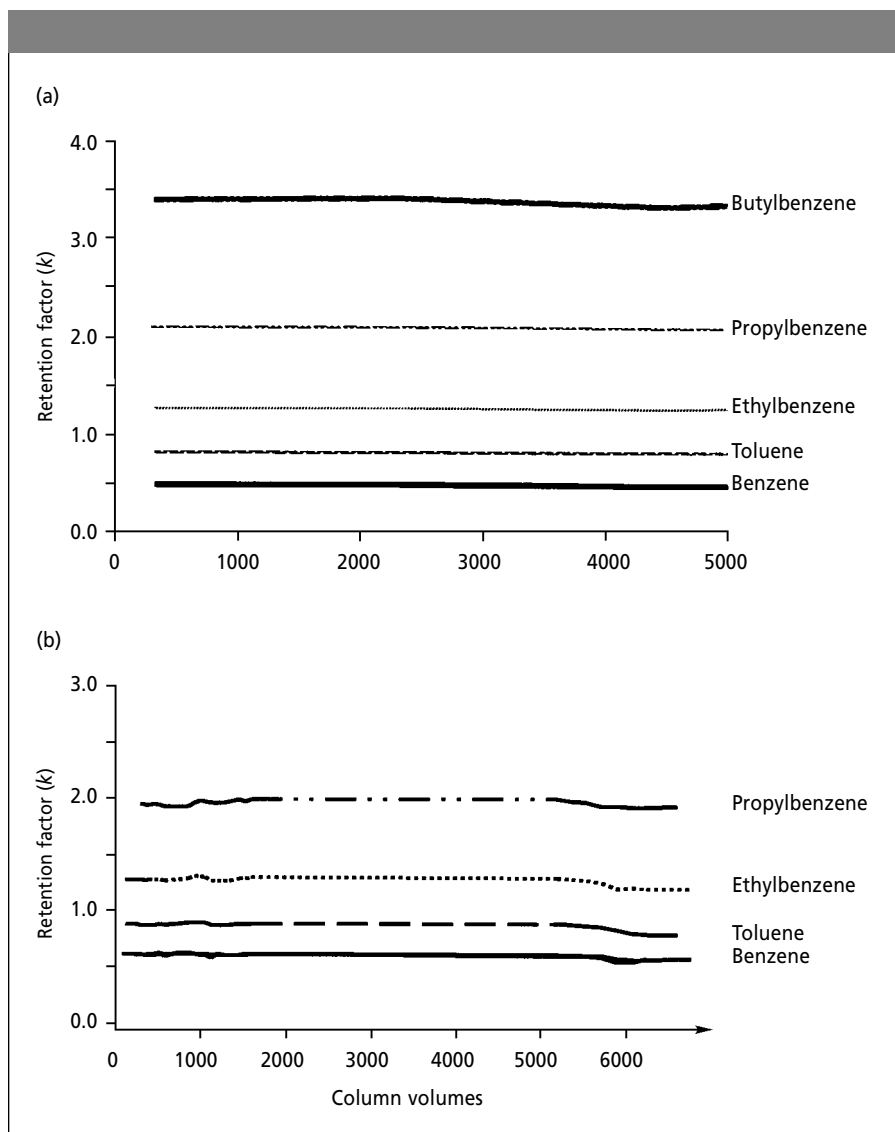
Figure 3: Analysis of the (a) chemical and (b) thermal stability of a polybutadiene-coated zirconia column. Conditions (a): wash fluid: 90:10 (v/v) 1 M sodium hydroxide in water–methanol (pH 14); mobile phase: 50:50 (v/v) acetonitrile–water; temperature: 35 °C. Conditions (b): mobile phase: 15:85 (v/v) acetonitrile–water; temperature: 195 °C. Column (a, b): 150 mm × 4.6 mm ZirChrom-PBD; flow rate (a, b): 1.0 mL/min.
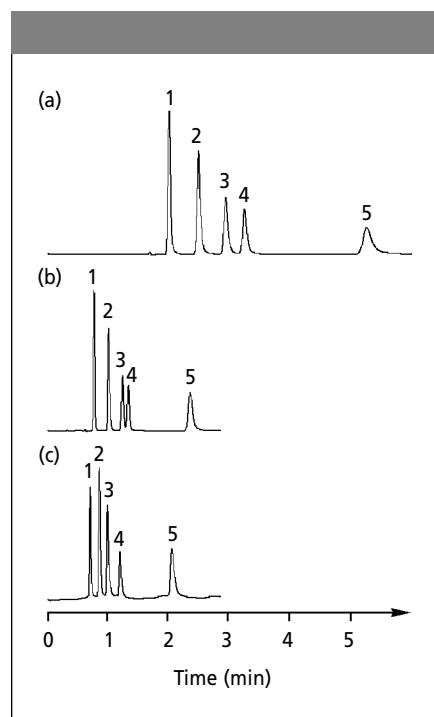
Figure 4: Separation of phenol and four of its chloroderivatives at column temperatures of (a) 30 °C, (b) 80 °C, and (c) 200 °C. Column: 150 mm × 4.6 mm ZirChrom-PBD; mobile phase: (a, b) 65:35 water–acetonitrile, (c) 100% water; flow rate: 3.0 mL/min; detection: UV absorbance at 254 nm. Peaks: 1 = phenol, 2 = 4-chlorophenol, 3 = 4-chloro-3-methyl phenol, 4 = 2,4,6-trimethylphenol, 5 = 2,4,6-trichlorophenol.

mated experimental error in the log k values (approximately 0.02 units in log k). For details concerning principal component analysis, refer to reference 46.

Results and Discussion

Column efficiency: Table II lists the number of theoretical plates for all 27 test analytes on each of the five columns. Each column type is characterized by two global figures of merit: the average and median plate counts for all analytes. The polybutadiene-coated zirconia and silica-based columns proved to be equally efficient overall for these 27 probe molecules, with both having a mean reduced plate height of 5.5. The alumina-based, graphitized carbon–clad zirconia, and polymeric phases had mean reduced plate heights of 6.8, 19, and 26, respectively.

Each column exhibited a fairly wide range of plate counts for the different solutes, but the polymer phase gave consistently and considerably lower plate counts than the silica-, alumina-, or zirconia-based phases. The polybutadiene-coated zirconia phase showed the best reduced plate height for the maximum and minimum plate count compared with the other phases. This very high efficiency results in part from the small (3-μm d_p), highly monodisperse size of these particles and from the fast solute mass transfer that can occur within the thin layer of cross-linked polybutadiene as opposed to a purely polymeric phase. Figure 6 compares the chromatographic efficiency of the polybutadiene-coated zirconia phase column with that of two purely polymeric phases for separating three alkylparabens. Generally, the polymeric columns share the pH stability of zirconia-based columns, but they have poor column efficiency even for small molecules such as these.

Chromatographic selectivity: Next, we investigated differences in retention selectivity for the 27 probe analytes on the five test columns. Specifically, we compared the analytes' retention factors (k) on the silica-based column with their selectivity on the other four columns. Although endcapping, carbon load, and silica purity affect retention and band spacing for different bonded-phase C18 silica columns, they rarely cause major changes in band spacing of nonelectrolytes, as long as all other chromatographic conditions are the same. Thus, we believe our comparison of selectivity differences between these five stable columns is indicative of global differences between the different substrates in relation to most silica-based, C18 reversed-phase materials.

Based on the manufacturers' data, we anticipated a fairly wide range in the amount of stationary phase — and thus, phase ratios — among these materials, and we anticipated that it would be reflected in a broad range of k values. The selectivity data in Figure 7 are presented as the ratio of k for any given solute to that of benzene, which should normalize the phase ratios. The polybutadiene-coated zirconia and silica-based columns show very similar chemical selectivity for this chemically diverse range of probe solutes (Figure 7a). The main differences in selectivity are for pyridine (analyte 14) and N,N-dimethylaniline (analyte 16). Both of these compounds are basic and positively charged under the experimental mobile-phase conditions, and it is well known that the adsorption of phosphate from the eluent imparts a negative charge to the surface of zirconia-based stationary phases. This charge results in greater retention of positively charged species on the polybutadiene-coated zirconia phase column because of mixed-mode reversed-phase and cation-exchange retention processes (33,34). Recent work in our laboratory showed that
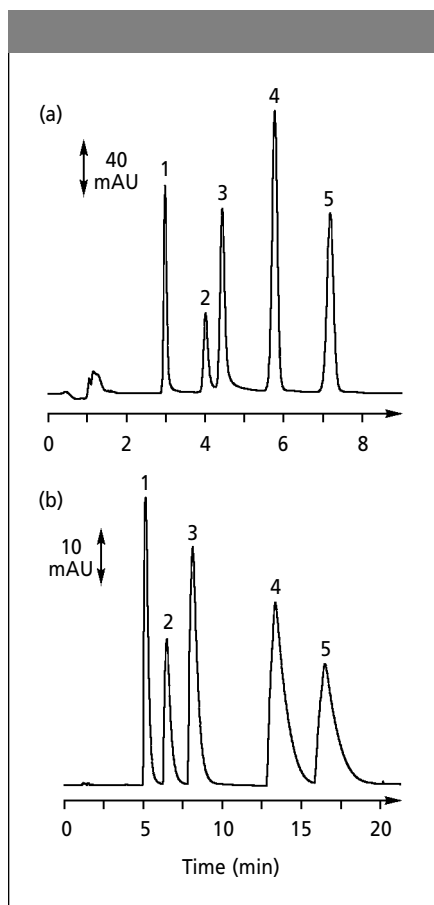
Figure 5: Separation of five tricyclic antidepressants on (a) polybutadiene-coated zirconia and (b) C18 silica columns. Mobile phase: (a) 45:55 (v/v) acetonitrile–20 mM potassium phosphate (pH 12.0), (b) 50:50 (v/v) acetonitrile–20 mM potassium phosphate (pH 7); flow rate: 1.0 mL/min; temperature: 30 °C; detection: UV absorbance at 254 nm. Peaks: 1 = nordoxepin, 2 = protriptyline, 3 = nortriptyline, 4 = imipramine, 5 = amitriptyline.

Table I: General characteristics of the five reversed-phase LC test columns*

Description	Graphitized Carbon–Clad Zirconia†	C18 Silica	Polymeric	Polybutadiene-Coated Alumina	Polybutadiene-Coated Zirconia‡
Particle size (μm)	3	3.5	5	5	3
Pore size (Å)	300	300	100	80	300
Column size (mm × mm)	150 × 4.6	150 × 4.6	150 × 4.6	150 × 4.6	150 × 4.6
Low pH limit	0.5	1.8	1	1.3	0.5
High pH limit	14	8	14	12	14
Temperature limit (°C)	200	80	150	†	200
Carbon loading (% carbon)	1.1	2.8	§	2.0	3.0

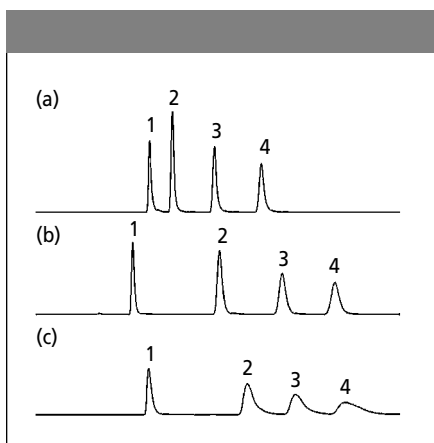* Specifications as reported by manufacturer at the time the study was performed.
† ZirChrom-Carb (ZirChrom Separations).
‡ ZirChrom-PBD (ZirChrom Separations).
§ Data not available.

		Graphitized Carbon–Clad Zirconia	C18 Silica	Polybutadiene-Coated Alumina	Polymeric	Polybutadiene-Coated Zirconia
Analyte	Solute					
1	Uracil	12	7.2	5.7	9.3	7.9
2	Benzyl formamide	11	6.0	5.7	8.2	7.3
3	Benzyl alcohol	7.0	5.6	5.6	8.7	6.1
4	Phenol	8.9	5.5	6.7	8.1	6.0
5	Benzoic acid	23	6.5	7.3	8.8	8.0
6	3-Phenylpropanol	8.1	5.9	8.7	23	7.8
7	Acetophenone	9.0	4.8	5.9	19	5.5
8	Benzonitrile	12	5.4	7.0	15	5.3
9	p-Chlorophenol	17	5.7	6.9	11	6.3
10	Methyl benzoate	16	4.7	6.4	27	5.5
11	Nitrobenzene	17	4.6	5.7	17	4.9
12	Anisole	7.9	4.5	7.2	21	4.7
13	Benzene	6.5	4.3	6.5	23	4.6
14	Pyridine	107	11	4.6	9.3	5.0
15	p-Nitrotoluene	19	4.5	5.9	25	4.7
16	N,N-Dimethylaniline	10	8.3	5.2	57	5.4
17	p-Nitrobenzyl chloride	9.4	4.5	6.2	23	4.8
18	Toluene	7.7	4.3	7.2	26	4.5
19	4-Butylbenzoic acid	24	5.4	7.4	16	8.3
20	Benzophenone	9.5	4.4	6.6	76	5.3
21	Bromobenzene	19	4.6	5.5	25	4.1
22	Ethyl benzene	10	4.6	7.2	27	4.2
23	p-Xylene	5.6	4.9	5.6	33	4.1
24	Naphthalene	92	4.7	6.4	68	4.5
25	p-Dichlorobenzene	17	5.0	5.8	46	4.0
26	Propylbenzene	13	5.2	10	34	5.0
27	Butylbenzene	23	6.2	15	35	6.0
	Mean	**19**	**5.5**	**6.8**	**26**	**5.5**
	Median	**12**	**5.0**	**6.4**	**23**	**5.3**
	Lowest*	**5.6**	**4.3**	**4.6**	**8.1**	**4.0**
	Highest†	**107**	**11**	**15**	**76**	**8.3**

Table II: Reduced plate height for 27 analytes on the five test columns

Figure 6: Separation of three alkylparabens on (a) a polybutadiene-coated zirconia column, (b) a polymeric column, and (c) a second polymeric column. Column dimensions: 150 mm × 4.6 mm; mobile phase: (a)10:10:20:60 (v/v/v/v) methanol–acetonitrile–tetrahydrofuran–water, (b, c) 10:20:30:40 (v/v/v/v) methanol–acetonitrile–tetrahydrofuran–water; flow rate: 1.0 mL/min; temperature: 50 °C; injection volume: 2.0 μL; detection: UV absorbance at 254 nm; column plate numbers: (a) 12,000, (b) 7000, (c) 1000. Peaks: 1 = uracil, 2 = ethylparaben, 3 = propylparaben, 4 = butylparaben.

the loading capacity of polybutadiene-coated zirconia phase for positively charged drugs is three- to fourfold greater than that of many conventional columns (47).

Similarly, the polybutadiene-coated alumina phase shows selectivity very similar to that of the silica-based phase under these conditions (Figure 7b); however, the overall retention on the polybutadiene-coated alumina column is very low, which likely is due to a much lower stationary-phase loading. As for the polybutadiene-coated zirconia and polybutadiene-coated alumina phases, the adsorption of phosphate onto the surface through a Lewis acid–base reaction induces a net negative charge on the phase (34), which leads to the high retention of cationic pyridine and N,N-dimethylaniline. Figure 7c illustrates the more varied retention properties of the polymer phase compared with those of the silica phase. Although the general retention trend is similar on both columns, the elution order often is different. Finally, Figure 7d compares the selectivity of the test solutes on the graphitized carbon–clad zirconia column with the selectivity of the silica-based column. Of the four columns tested, the

graphitized carbon–clad zirconia phase had the most markedly different selectivity from that of the silica phase. This result is as expected, in that the column's graphite-like layered stationary phase is rigid and cannot accommodate partitioning into a bonded phase or polymeric stationary phase matrix (44). Figure 8 illustrates one practical outcome — the successful separation of two aromatic diastereomers on the graphitized carbon–clad zirconia column. This separation cannot be achieved on a conventional C18 silica column, despite its higher efficiency: The inability of solutes to partition into the rigid carbon phase causes its chemical selectivity for different geometric isomers (41).

Figure 9 and Table III show the selectivity differences between the various phases and their global similarity to the C18 silica phase from a different perspective — in log k–log k plots. Horváth (45) developed these plots to study similarities in retention energetics on different types of reversed phases. High correlation coefficients and slopes close to unity indicate near identity of retention thermodynamics for the two phases. The correlation coefficients (r^2) of 0.980 and 0.978 for the

polybutadiene-coated zirconia phase and polybutadiene-coated alumina, respectively, show that they are most similar to the C18 silica phase with respect to retention processes. The very weak correlation (r^2 of 0.529) between the graphitized carbon–clad zirconia and silica column show that they are most dissimilar. The polymer phase occupies a position intermediate between the polymer-coated metal oxides and the carbon-coated zirconia. The amine solutes were not considered in the analysis.

Hydrophobic interactions: One of the key characteristics that classifies a particular material as a reversed phase and that can distinguish it from other reversed-phase materials is the existence of a linear relationship between log k and the number of methylene units in a homolog series. Figure 10 presents these data for a series of n-alkylbenzene homologs that serve as prototypical hydrophobic, nonpolar analytes. The plots indicate that absolute retention of these nonpolar solutes differs greatly among the five phases. Clearly, retention is greatest on the polymeric phase followed by the C18 silica, the graphitized carbon–clad zirconia, and the polybutadiene-coated zirconia phases. Retention on the polymeric polybutadiene-coated alumina phase is very low, supporting our statement above that the material has only a small amount of polymer present.

However, absolute retention, as represented by the vertical position in Figure 10 and the magnitude of k, is not necessarily the best index of phase hydrophobicity. The free energy of retention can be related to k as:

$$\Delta G^\circ = -RT(\ln[k/\phi]) \qquad [1]$$

where R is the gas constant, T is the temperature in kelvins, and ϕ is the phase ratio. The slopes of the linear regression lines in Figure 10 are proportional to the free energy of transfer of a methylene group from the mobile phase to the stationary phase. This relationship is shown directly in equation 2:

$$\Delta G^\circ_{meth} = -RT(\ln[k_{n+1}/k_n]) \qquad [2]$$

where k_{n+1} and k_n denote the capacity factors of the nth and nth + 1 homologs. The slopes for each of the five stationary phases are as follows: −0.583 kJ/mol for the polymeric phase, −0.880 kJ/mol for the C18 silica, −0.887 kJ/mol for the graphitized carbon–clad zirconia phase, −0.826 kJ/mol for the polybutadiene-coated zirconia
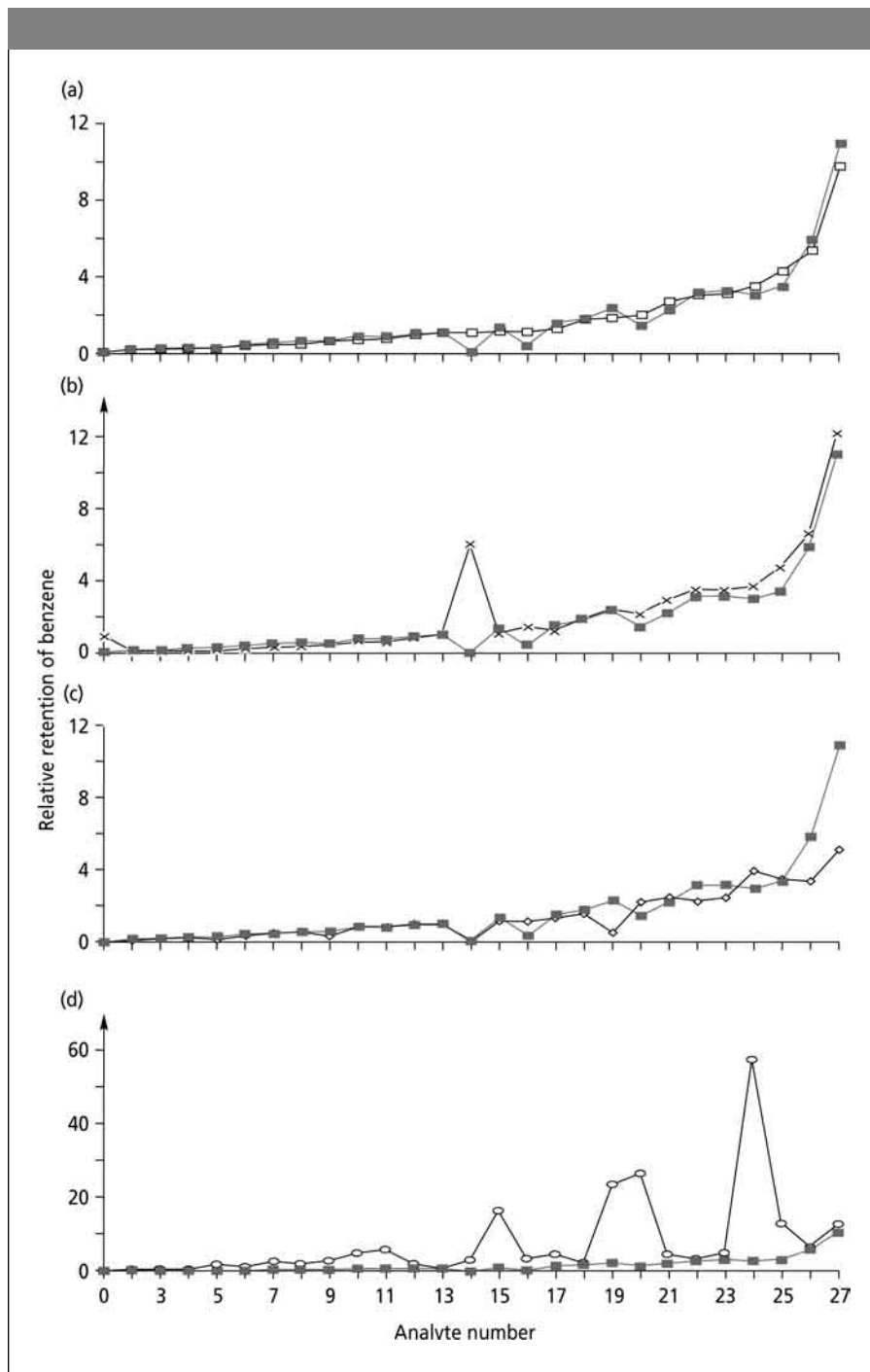
Figure 7: Selectivity comparison of normalized phase ratios ($k_{solute}/k_{benzene}$) between a C18 silica column (■) and four nonsilica reversed-phase columns: (a) polybutadiene-coated zirconia (□), (b) polybutadiene-coated alumina (×), (c) polymeric (◇), and (d) graphitized carbon–clad zirconia (○). Mobile phase: 40:60 (v/v) acetonitrile–50 mM phosphate (pH 3.2); flow rate: 1.0 mL/min; temperature: 21 °C; detection: UV absorbance at 254 nm. Analytes 1–27 are identified in Table II.

phase, and −0.906 kJ/mol for the polybutadiene-coated alumina phase. Thus, all but the polymer phase have similar hydrophobicities as assessed through the free energy of retention of a methylene group.

Principal component analysis of retention factor data: Last, we conducted a principal component analysis of the retention data to fully compare retention in these five

phases — both among themselves and as compared with five conventional silica-based bonded phases (for example, C18 and C8) for which a principal component analysis was previously reported (48). A principal component analysis does not impose any preconceived model of retention. We omitted analytes 1, 2, 5, 14, 16, and 19 to allow

a direct comparison with the results from the previous silica study. The results of the analysis show that four principal components are required to describe 99.96% of the variability in the retention data set (see Table IV). In contrast, results from the study of five silica-based reversed-phase columns show that only one principal component is required to describe 99.92% of the total variance in the retention factor data (48). In the previous study, all of the correlation coefficients for the log k versus log k plots were 0.997 or better, which indicated very similar retention behavior for the same 21 probe molecules on these silica columns.

The differences among the five columns in our study was even more apparent when the columns were plotted using the scores of the first two principal components. The graphitized carbon–clad zirconia and polybutadiene-coated alumina columns emerged as the most distinct (see Figure 11). The principal component analysis results suggested that intermolecular inter-

actions for the analytes on the five chemically distinct columns in our study differ from one another in a more complex way than they do on conventional reversed-phase silica phases.

Conclusions

Advances in the chemical and thermal stability of HPLC column packing materials allow for the use of mobile-phase conditions and column temperatures that previously had been unreachable with silica-based stationary phases. The practical benefits of these more stable chromatographic materials range from the ability to use harsh cleaning conditions for column regeneration to analysis speeds as much as an order of magnitude faster. Moreover, chromatographers can greatly reduce or even eliminate organic waste generation at elevated column temperatures.
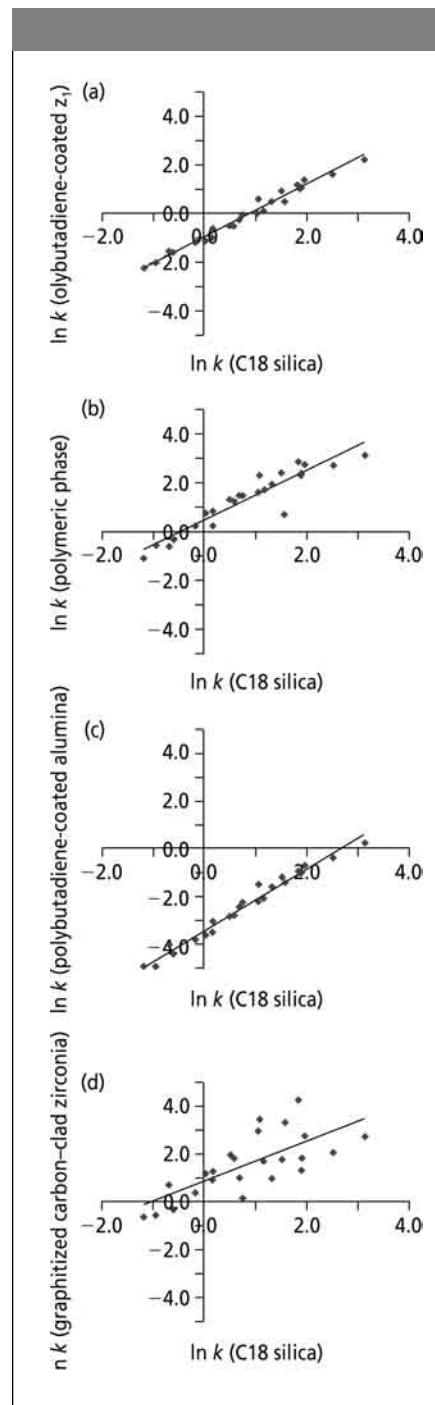
Our comparison of five distinct columns that exhibit varying degrees of chemical and thermal stability showed that the polybutadiene-coated zirconia phase column was the most efficient, and the polymeric column
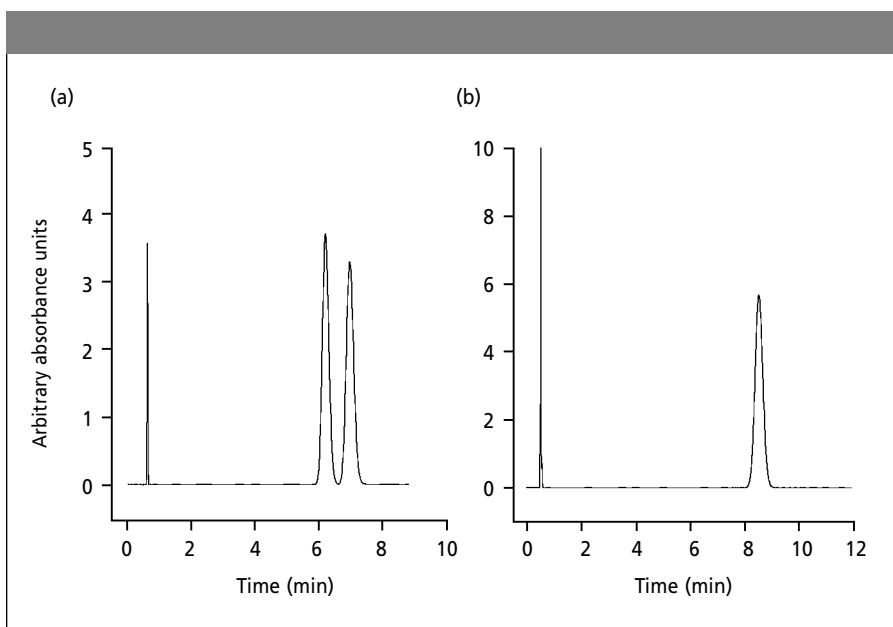
Figure 8: HPLC analysis of two aromatic diastereomers, (R)-Mosher-(±)-warfarin, on 50 mm × 4.6 mm (a) graphitized carbon–clad zirconia and (b) C18 silica columns. Mobile phase: (a) 45:55 (v/v) tetrahydrofuran–water, (b) 40:60 (v/v) tetrahydrofuran–water; flow rate: 1.0 mL/min; temperature: ambient; detection: UV absorbance at 254 nm.
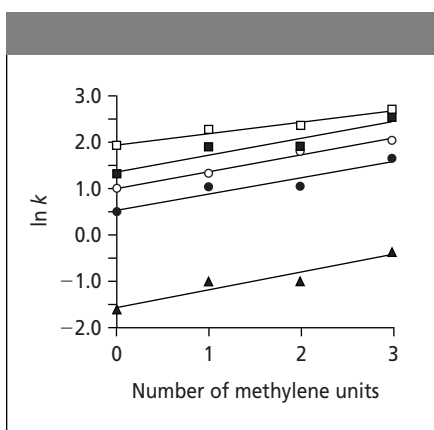

Figure 9: Comparison of retention thermodynamics between a C18 silica phase and four nonsilica phases. Mobile phase: 40:60 (v/v) acetonitrile–50 mM phosphate (pH 3.2); flow rate: 1.0 mL/min; temperature: 21 °C; detection: UV absorbance at 254 nm. Table III lists the regression statistics for each plot.

Table III: Regression statistics for Figure 9				
Plot	Column	Slope	Intercept	Correlation Coefficient
a	Polybutadiene-coated zirconia	1.070 ± 0.0323	−0.954 ± 0.045	0.980
b	Polymeric phase	1.000 ± 0.0816	0.462 ± 0.11	0.874
c	Polybutadiene-coated alumina	1.290 ± 0.0413	−3.410 ± 0.057	0.978
d	Graphitized carbon–clad zirconia	0.829 ± 0.176	0.853 ± 0.230	0.529

was the least efficient. In terms of chromatographic selectivity for nonelectrolytes, the polybutadiene-coated zirconia phase and polybutadiene-coated alumina columns were very similar. In contrast, the graphitized carbon–clad zirconia column showed the greatest difference in reversed-phase chemical selectivity of any of the columns tested compared with the C18 silica column. Practically speaking, the graphitized carbon–clad zirconia column should be used to get the largest change in reversed-phase chemical selectivity when a separation does not work on a more traditional reversed-phase material. The principal component analysis study revealed that four principal components are necessary to describe retention on the five columns, compared with one principal component for five analogous reversed-phase silica columns. This result suggests a more complicated mode of retention for this next generation of stable HPLC columns.

Figure 10: Plot of ln *k* versus number of methylene units for a series of *n*-alkylbenzene homologs. Columns: □ = polymeric, ■ = C18 silica, ○ = graphitized carbon–clad zirconia, ● = polybutadiene-coated zirconia, ▲ = polybutadiene-coated alumina. Mobile phase: 40:60 (v/v) acetonitrile–50 mM phosphate (pH 3.2); flow rate: 1.0 mL/min; temperature: 21 °C; detection: UV absorbance at 254 nm.
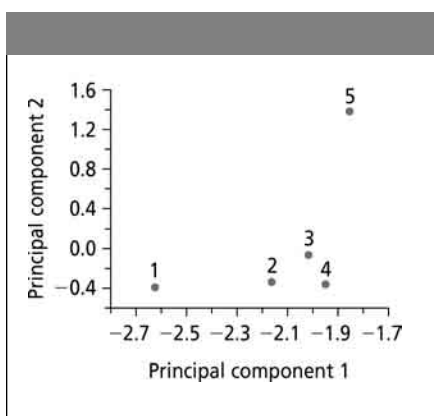
Figure 11: Principal components analysis scores plot for the five test columns. Columns: 1 = polybutadiene-coated alumina, 2 = polybutadiene-coated zirconia, 3 = polymeric, 4 = C18 silica, 5 = graphitized carbon–clad zirconia.

References

(1) J.J. Kirkland, M.A. van Straten, and H.A. Claessens, *J. Chromatogr. A* **797,** 111–120 (1998).
(2) J.J. Kirkland, J.W. Henderson, J.J. DeStefano, M.A. van Straten, and H.A. Claessens, *J. Chromatogr. A* **762,** 97–112 (1997).
(3) R.K. Iler, *The Chemistry of Silica* (John Wiley & Sons, New York, 1979).
(4) F.D. Antia and Cs. Horváth, *J. Chromatogr.* **435,** 1–15 (1988).
(5) J.W. Li and P.W. Carr, *Anal. Chem.* **69,** 2202–2206 (1997).
(6) J.W. Li and P.W. Carr, *Anal. Chem.* **69,** 2550–2553 (1997).
(7) P.L. Zhu, J.W. Dolan, and L.R. Snyder, *J. Chromatogr.* **756,** 41–50 (1996).
(8) L.R. Snyder, *J. Chromatogr.* **689,** 105–115 (1997).
(9) S.B. Hawthorne, Y. Yang, and D.J. Miller, *Anal. Chem.* **66,** 2912–2920 (1994).
(10) R.M. Smith and R.J. Burgess, *J. Chromatogr. A* **785,** 49–55 (1997).
(11) R.M. Smith and R.J. Burgess, *Anal. Comm.* **33,** 327–329 (1996).
(12) D.J. Miller and S.B. Hawthorne, *Anal. Chem.* **69,** 623–627 (1997).
(13) J.J. Kirkland, J.L. Glajch, and J. Kohler, *J. Chromatogr.* **384,** 81–90 (1987).
(14) J.R. Benson and D.J. Woo, *J. Chromatogr. Sci.* **22,** 386–396 (1984).
(15) H. Engelhardt, H.A. Mottola, and J.R. Steinmetz, in *Chemically Modified Surfaces,* H.A. Mottola and J.R. Steinmetz, Eds. (Elsevier, Amsterdam, 1992), pp. 225.
(16) J.E. Haky, A. Raghani, and B.M. Dunn, *J. Chromatogr.* **541,** 303–316 (1991).
(17) U. Trudinger, G. Muller, and K.K. Unger, *J. Chromatogr.* **535,** 111–125 (1990).
(18) L.R. Snyder, J.L. Glajch, and J.L. Kirkland, *Practical HPLC Method Development* (John Wiley & Sons, New York, 1988), pp. 41–46.
(19) R.E. Majors, *LCGC* **15**(11), 1008–1015 (1997).
(20) J. Knox, and B. Kaur, *Eur. Chromatogr. News* **1,** 12–14 (1987).
(21) K. Unger, *Anal. Chem.* **55,** 361A–375A (1983).
(22) K. Unger, *Porous Silica* (Elsevier, Amsterdam, J. Chromatogr. Library vol. 16, 1977).
(23) K. Unger, A. Kurganov, V. Davankov, T. Isajeva, K. Unger, and F. Eisenbeiss, *J. Chromatogr.* **660,** 97–111 (1994).
(24) M.P. Rigney, T.P. Weber, and P.W. Carr, *J. Chromatogr.* **484,** 273 (1989).
(25) M.P. Rigney, E.F. Funkenbusch, and P.W. Carr, *J. Chromatogr.* **499,** 291 (1990).
(26) L. Sun, A.V. McCormick, and P.W. Carr, *J. Chromatogr.* **658,** 465 (1994).
(27) L. Sun and P.W. Carr, *Anal. Chem.* **67,** 2517 (1995).
(28) T.P. Weber, P.W. Carr, and E.F. Funkenbusch, *J. Chromatogr.* **519,** 31 (1990).
(29) T.P. Weber and P.W. Carr, *Anal. Chem.* **62,** 2620 (1990).
(30) J.A. Blackwell and P.W. Carr, *J. Chromatogr.* **549,** 43 (1991).
(31) J.A. Blackwell and P.W. Carr, *J. Chromatogr.* **549,** 59 (1991).
(32) J.A. Blackwell and P.W. Carr, *J. Liq. Chromatogr.* **14,** 2875 (1991).
(33) W.A. Schafer, P.W. Carr, E.F. Funkenbusch, and C.A. Parson, *J. Chromatogr.* **587,** 137 (1991).
(34) W.A. Schafer and P.W. Carr, *J. Chromatogr.* **587,** 149 (1991).
(35) J.A. Blackwell and P.W. Carr, *Anal. Chem.* **64,** 853 (1992).
(36) C. McNeff and P.W. Carr, *Anal. Chem.* **67,** 2350–2353 (1995).
(37) M.H. Glavanovich and P.W. Carr, *Anal. Chem.* **66,** 2584 (1994).
(38) C.V. McNeff, U. Zhao, and P.W. Carr, *J. Chromatogr.* **684,** 201 (1994).
(39) C. McNeff, Q. Zhao, E. Almlöf, M. Slickinger, and P.W. Carr, *Anal. Biochem.* **274,** 181–187 (1999).
(40) J. Li and P.W. Carr, *Anal. Chem.* **69,** 2202–2206 (1997).
(41) P.T. Jackson and P.W. Carr, *ChemTech* **X,** 29–37 (1998).
(42) R.E. Majors, *LCGC* **15**(3), 220–237 (1997).
(43) M.P. Rigney, Ph.D. thesis, University of Minnesota, Minneapolis, Minnesota (1989).
(44) T.P. Weber, P.T. Jackson, and P.W. Carr, *Anal. Chem.* **67,** 3042–3050 (1995).
(45) R.J. Steffeck, S.L. Woo, R.J. Weigand, and J.M. Anderson, *LCGC* **13**(9), 720–726 (1995).
(46) E.R. Malinowski, *Factor Analysis in Chemistry* (John Wiley & Sons, New York, 2nd ed., 1991).
(47) "ZirChrom-PBD: Stable, Efficient, Reversed-Phase with Good Peak Shape for Basic Drugs," ZirChrom Technical Bulletin #190, ZirChrom Separations Inc. (Anoka, Minnesota, 1999).
(48) L. Tan, Ph.D. thesis, University of Minnesota, Minneapolis, Minnesota (1994). ■

Table IV: Results of principal components analysis of retention factor data

Number of Principal Components	Eigenvalue	Variance (%)	Total Variance (%)	Residual Standard Deviation
1	22.960	89.929	89.929	0.175
2	2.341	9.168	99.096	0.061
3	0.157	0.615	99.711	0.042
4	0.063	0.246	99.957	0.023
5	0.011	0.043	100.000	0.000